Low Temperature Physics/Fizika Nizkikh Temperatur, 2019, v. 45, No. 6, pp. 710–721

VUV Photolysis of CH_4–H_2O mixture in methane-rich ices: Formation of large complex organic molecules in astronomical environments

Lahouari Krim and Mindaugas Jonusas

Sorbonne Université, CNRS, De la Molécule aux Nano-Objets: Réactivité, Interactions, Spectroscopies MONARIS, 75005, Paris, France
E-mail: Lahouari.krim@upmc.fr

Received January 4, 2019, published online April 26, 2019

The present work aims to highlight the influence of water molecules in the photo-decomposition of methane ice and reveal the photoproducts formed in solid phase upon VUV irradiation of CH_4–H_2O mixture in methane-rich ices. The analysis of our IR spectra shows that even with very low concentrations of water in methane ices, several oxygenated hydrocarbons are formed as photoproducts derived from the photodecomposition of water and methane at cryogenic temperatures. We show that both alka[e]nes and oxygen bearing organics are efficiently formed at temperatures as low as 3 K. However, while the IR signatures of the alka[e]nes such as C_2H_6, C_2H_4 and C_2H_2 dominate the IR spectra of the irradiated CH_4–H_2O ices at temperatures lower than 50 K, the heating of the sample to 110 K reveals the formation of large carbon chain complex organic molecules such as ethanol, pronanol, propanal and glycolaldehyde.

Keywords: astrochemistry, laboratory simulation, IR spectroscopy, complex organic molecules.

Introduction

Saturated and unsaturated hydrocarbons are likely formed in aerosol particles of CH_4-rich atmospheres of planets and moons such as Saturn and Saturn's huge moon Titan. The icy surfaces of some solar objects such as Pluto, Saturn and Titan may host giant dunes of hydrocarbons like methane and ethane ice dunes which have been reported through images [1] from the New Horizons flyby of Pluto in July 2015. Additionally, methane and ethane mixed ice clouds are both present in the troposphere and stratosphere of Titan atmosphere [2]. In this sense, photochemistry of methane ices has been investigated by several groups in pure methane and rare gas matrices in order to explore the formation routes of carbon chains and hydrocarbon detected towards planetary atmospheres and molecular clouds. Wu *et al.* [3] studied, using synchrotron vacuum-ultraviolet light, the photolysis of methane dispersed in solid neon. They showed that carbon chains up to five carbon atoms are easily formed at cryogenic temperatures and might be part of the chemical composition of methane rich regions in space.

Similar investigations carried out by Lin *et al.* [4] underlined the formation of large carbon chains up to 20 carbon atoms and other various radical saturated and unsaturated hydrocarbons. The cryogenic synthesis of CH, CH_2, CH_3, C_2H_2, CH_2H_3, C_2H_4, C_2H_5 and C_2H_6 has been examined by Bennett *et al.* [5] through energetic electrons irradiation of pure methane ices to mimic the role of cosmic-ray particles in the chemical transformation of methane which can be the source of large complex molecules including prebiotic species [6]. Laboratory studies of methane ice photolysis have been extended to molecular ices relevant to cometary and interstellar ices and also to icy satellites of planetary systems in order to identify the complex organic molecules formed in astronomical environments.

Several studies have been focused in photolysis and radiolysis of CH_4–H_2O mixed ices to probe the formation of oxygen bearing species already detected or looked for in space such as ethanol (C_2H_5OH), dimethyl ether (CH_3OCH_3) [7], methyl acetate (CH_3COOCH_3) [8], ethyl formate (C_2H_5OCHO) [8] and glycolaldehyde ($HOCH_2CHO$) [9]. Moore *et al.* [10,11] highlight radiation experiments in H_2O-rich ices containing astrochemical species relevant such as CO, C_2H_2 and CH_4. They identified many complex species which depend strongly on the chemical composition of the irradiated ices.

In the case H_2O–CH_4 mixed ices, three H_2O-rich ices with different H_2O:CH_4 concentrations, 2:1, 7:1, and 15:1, have been considered. The IR spectra recorded after irradiation showed the formation of C_2H_6, C_3H_8, CH_3OH,

C_2H_5OH, H_2CO, CH_3CHO in addition to CO and CO_2. Although the H_2O:CH_4 concentrations have been specifically chosen based on astronomical detections where CH_4 is highly less abundant than water; Bockelee-Morvan *et al.* [12] reported from Rosetta observations that in the coma of comet 67P, methane abundance relative to water is ranged between 0.2 and 0.5%; these laboratory simulations carried out in order to provide significant data correlating to such observations, cannot reveal the nature of all chemical species formed during the photo processing of CH_4–H_2O mixed ices in water-rich environment configuration. In fact even in the case of experiments performed with the lowest concentration of water (H_2O:CH_4 = 2:1), the IR spectra recorded by Moore and Hudson are dominated by the huge wide absorption bands of water ice which hide many reaction products formed during the photolysis processing.

In order to study the influence of H_2O molecules in the photo-induced decomposition of CH_4 in solid phase, we have investigated the photolysis of CH_4–H_2O mixed ices in CH_4-rich environments. Counter to H_2O-ice which has strong absorption signals in practically all the MID–IR spectral region; the H_2O-twisting mode IR signal is expanded in the 500–1000 cm^{-1} spectral region, H_2O-bending mode absorb in a wide spectral range 1400–1700 cm^{-1} and the 2800–3700 cm^{-1} spectral region is congested by the huge absorptions of OH vibrations; the IR absorption signals of CH_4-ice, even with very high concentration of methane, consist of two main relative narrow bands at 1301 and 3012 cm^{-1}. Consequently, the isolation of H_2O + CH_4 photo-induced solid state reaction in methane-rich environment will allow a better identification of the reaction products derived from the simultaneous solid state decomposition of H_2O and CH_4.

Experimental section

The experimental setup used in the present study has already been described in previous articles [13], thus only important features are mentioned hereafter. The experiments are performed under ultra high vacuum at 10^{-10} mbar. A Rh-plated copper mirror is used as a substrate to condense the reactants and to form the CH_4–H_2O mixed ices. CH_4 (99.999%) purchased from Messer and demineralized and degassed H_2O are co-condensed pure at 3 K. The photolysis of our samples during 30 min, have been performed using a VUV lamp with a flux around 10^{15} photons·cm^{-2}·s^{-1} (Hamamatsu L10706 UV) and photon outputs of 25% at 121 nm (~10.3 eV) and 75% at 160 nm (~7.7 eV).

The infrared spectra of the solid samples before and after photolysis are recorded using a Bruker Vertex 80v Fourier infrared (FTIR) spectrometer in transmission–reflection mode. The sample thickness and the exact amount of CH_4 and H_2O forming the ice have been evaluated, as it will be discussed in the result section, from the IR spectra of CH_4-rich ices by calculating the column densities (molecule·cm^{-2}) of CH_4 and H_2O. Additionally, IR spectra of pure, methanol, ethanol, propanol and propanal ices have been recorded under the same experimental conditions and taken as reference spectra to characterize the reaction products which may derive from the irradiation of CH_4-rich ices containing water.

In order to reduce the recombination between the photoproducts derived from CH_4 and H_2O dissociations and avoid the formation of hydrated complexes trapped in CH_4-matrix, all the photolysis experiments have been carried out at the lowest temperature reached with our experimental setup that is 3 K. However, the goal of the present work is not to assign all the IR signals of the species formed after photolysis and trapped in CH_4-matrix at 3 K but to have an IR spectrum of heavy oxygenated species which would form through the photo-induced solid state reaction involving H_2O and CH_4. In fact, in addition to promote radical-radical reactions similar to those occurring at the surface of astronomical icy grains, the heating of the irradiated CH_4–H_2O ices from 3 to 110 K allows to remove all alka[e]nes and to reveal the IR signatures of large carbon chain complex organic molecules without being hindered by the absorption bands of water ice. Such IR signatures are very important to be compared to references spectra of astronomically relevant large hydrocarbons.

Results and discussion

As the present study is devoted to emphasize the influence of water molecules in the photo-decomposition of the solid methane, one should pay attention on the main photoproducts realized from the irradiation of methane ice which has been largely investigated previously [4,5,14]. As mentioned in the introduction part, many laboratory simulations of energetic decomposition of pure methane ice have been explored in order to underline the role of CH_4 fragmentation in the formation of complex organic molecules on the surfaces of icy bodies in the interstellar medium, comets and solar system objects.

In this context, using infrared absorption signatures to indentify the photoproducts, Lin *et al.* [4] showed that pure methane ices and methane dispersed in solid neon at 3 K subjected to irradiation at wavelengths less than 165 nm lead to the formation of CH_3, C_2H_2, C_2H_3, C_2H_4, C_2H_6, C_4H_2, C_4H_4, C_5H_2, C_8H_2 and C_nH with n = 1−5. They also showed that the adding of small amount of H_2 into solid neon enhanced the formation of long carbon chains C_n species, with n = 3−20. Bennett *et al.* [5] showed that pure methane ices irradiated at 10 K with energetic electrons lead mainly to the formation of CH, CH_2, CH_3 and C_2H_2, C_2H_3, C_2H_4, C_2H_5 and C_2H_6. Vasconcelos *et al.* [14] have confirmed, using ions bombardment of methane ice at 16 K, the formation of C_2H_2, C_2H_4, C_2H_6, C_3H_8, C_4H_8 and CH_3. However, they showed that CH_4 ices exposed to energetic radiations lead to the formation of propane C_3H_8

as the most abundant photoproduct contradicting previous laboratory results which showed that was ethane C_2H_6. They gave a yield ratio $[C_3H_8]/[C_2H_6]$ of the order of 20.

In order to reveal the new photoproducts formed upon UV irradiation in methane ices containing small amounts of water, methane-rich samples have been prepared by keeping the concentration of methane constant and varying that of water. Figure 1 shows the IR spectra of three CH_4-rich ices containing small amounts of water with concentrations of CH_4:H_2O = 3:1, 6:1 and 200:1. The assignments of all vibrational modes of CH_4–H_2O ice are directly reported in the figure [15].

The amounts of CH_4:H_2O concentrations have been evaluated from the IR spectra of CH_4-rich ices formed at 3 K. Even though the band strengths of molecular species depend strongly on the environment where they are trapped, we have preformed these column densities calculation in order to estimate the relative concentrations ratios $[CH_4]/[H_2O]$. The column densities n (molecule·cm^{-2}) of the CH_4 and H_2O can be deduced from the integrated IR intensities of the corresponding characteristic absorption bands [16].

In the case of water, the bending mode of H_2O at 1600 cm^{-1} has been used with the band strength of $1.2{\cdot}10^{-17}$ cm·molecules^{-1} taken from Gerakines *et al.* [17] investigations (the same value has been also predicted by DFT calculations for water monomer [18]). For the methane ice, as the samples are CH_4-rich ices, the CH_4 fundamental bands at 1306 and 3015 cm^{-1} are saturated, we have thus used the combination absorption band of CH_4 at 4202 cm^{-1} with the band strength [19] of $1.6{\cdot}10^{-18}$ cm·molecules^{-1} to estimate the amount of CH_4 in each sample. Knowing that CH_4 ice at cryogenic temperatures has a density [20] of 0.47 g·cm^{-3}, we have deduced the thickness of our samples around 1 μm. In such samples of methane ices containing small amounts of water, CH_4 molecules form a crystal where H_2O are entrapped.

Through this methane matrix isolation, we can distinguish the formation of many water clusters such as $(H_2O)_n$ where n = 1–6 as shown in Fig. 1. All these complexes absorb in the same spectral region for the bending mode at 1600 cm^{-1}, but they have their characteristic spectral positions in the OH stretching region, ranging from 3800 to 3100 cm^{-1}. The formation of water clusters in CH_4 matrix is in good agreement with the studies carried out by Yamakawa *et al.* [21]. However, we notice that in diluted sample with CH_4:H_2O concentration equal to 200:1, only water monomer has been detected (Fig. 1(a)). By increasing the amount of water in methane ice (Figs. 1(b) and 1(c)), we favor the formation of water aggregates. The samples containing water clusters (Figs. 1(b) and 1(c)) can also be characterized by monitoring the water aggregate libration through the huge and wide absorption band in the 900–600 cm^{-1} spectral region.

Figure 2 shows the global results of the photolysis of CH_4-rich ices containing different amounts of water. Many new signals appear in different spectral regions. The new signals are due to the photo fragments released from the photo-destruction of CH_4 and H_2O molecules as well as to reaction products formed through recombination between all the photo fragments. In addition to the formation of CO and CO_2 shown in Figs. 2(b), 2(d), 2(f) and which result from the oxidation of methane, other oxygen bearing organics such as alcohols and aldehydes are formed as photoproducts. However, many of the new signals observed in the IR spectra of the irradiated samples, shown in Figs. 2(b), 2(d), 2(f), have already been observed previously and as-

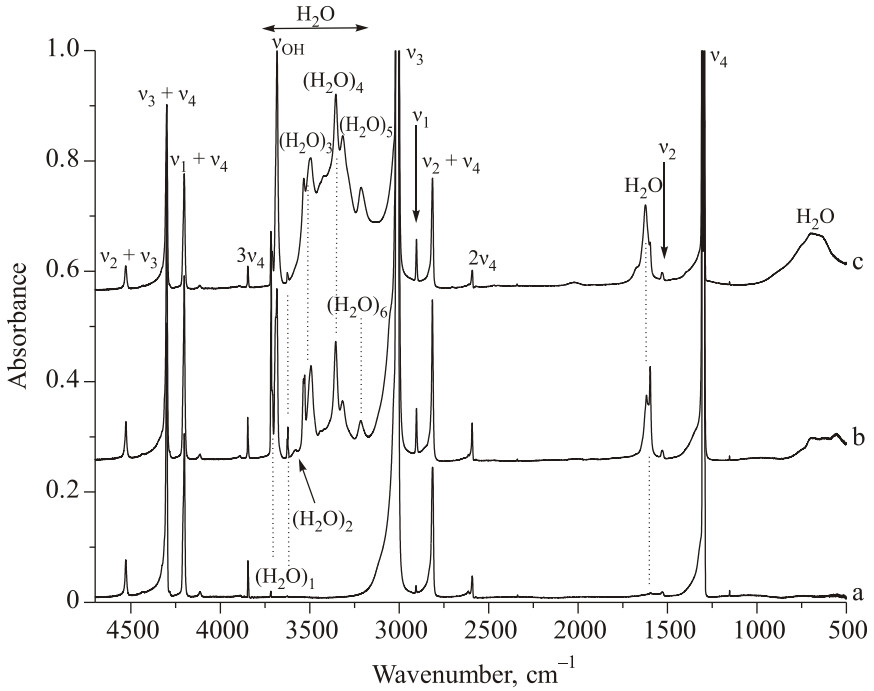

Fig. 1. IR spectra of CH_4-rich ices containing H_2O formed at 3 K with CH_4:H_2O concentrations equal to: 200:1 (a), 6:1 (b), 3:1 (c).

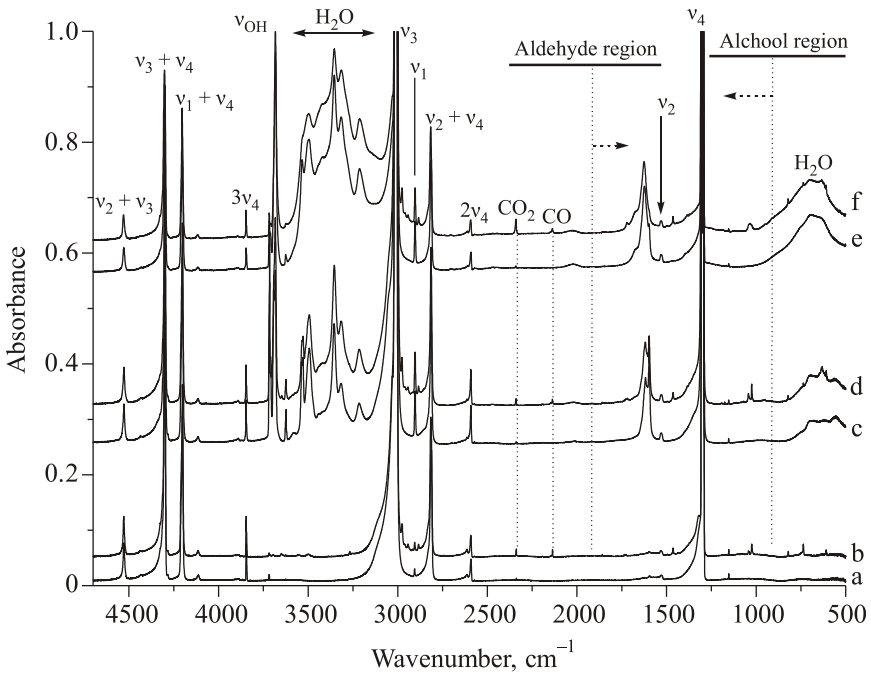

Fig. 2. IR spectra of CH_4-rich ices containing H_2O formed at 3 K, before and after UV photolysis: (a) $CH_4 + H_2O$ (200:1) ice; (b) $CH_4 +$ $+ H_2O$ (200:1) ice after UV photolysis; (c) $CH_4 + H_2O$ (6:1) ice; (d) $CH_4 + H_2O$ (6:1) ice after UV photolysis; (e) $CH_4 + H_2O$ (3:1) ice; (f) $CH_4 + H_2O$ (3:1) ice after UV photolysis.

signed to alka[e]nes which are proper photoproducts realized from methane such as C_2H_6, C_2H_4 and C_2H_2 absorbing strongly in the 500–1000 cm^{-1}, 1300–1500 cm^{-1} and 3200–2800 cm^{-1} spectral regions.

In order to characterize the reaction products formed during the CH_4–H_2O photolysis at 3 K we have analyzed the difference spectra before and after UV photolysis in 5 spectral regions:

i) C–O stretching region @ 1300–500 cm^{-1}: this region corresponds to the torsion modes of many alka[e]nes and also to the C–O stretching mode of many alcohols. This spectral region is shown in Fig. 3 and it will be used to characterize the different alcohols formed under our experimental conditions.

ii) H–C–H bending region @ 1500–1300 cm^{-1}: this region shown in Fig. 4, corresponds to the bending modes of many alkanes and alcohols.

iii) C=O functional group region @ 1900–1600 cm^{-1}: this region shown in Fig. 5 corresponds to many species with C=O functional groups such as HCO and H_2CO. It will be used to characterize species with carbonyl functional groups which might be formed under our experimental conditions.

iv) CO and CO_2 @ 2500–2100 cm^{-1}: the region of CO and CO_2 molecules already shown in Fig. 2, will not be discussed as CO and CO_2 are natural reaction products from CH_4 oxidation.

v) CH and OH stretching mode region @ the 3500–2800 cm^{-1}: This zone is dominated by the IR signals of $(H_2O)_n$, CH_4, C_2H_6 species and will be analyzed afterward during the heating of the sample, once all the alka[e]nes C_xH_y species, which desorb at temperatures lower than 80 K, are removed from the samples.

Figures 3 and 4 show the difference spectra before and after UV photolysis of CH_4-rich ices containing different amounts of water in the 1300–500 cm^{-1} and 1500–1300 cm^{-1} spectral regions, respectively. The analysis of the spectra from these two figures shows the formation of many alka[e]nes such as C_2H_6, C_2H_4, C_2H_2, C_3H_8 in addition to two radicals CH_3 and C_2H_5.

The spectral positions of all these species are in good agreement with previous experimental [4,5,14] studies devoted to CH_4 ice photolysis or radiolysis and showing that the photolysis of methane leads mainly to the formation of saturated and unsaturated hydrocarbons. The adding of water into CH_4 ice shows, in the difference spectra, new IR features due to the formation of oxygen bearing species. As the photolysis of methane ice leads mainly to long chain carbon species observed experimentally in Fig. 3 and as the adding of small mount water in methane ice brings additional reactants, during the photolysis of the sample, namely: H_2O, H, O, and OH species [22], we can suggest that species with several carbon atoms and one oxygen atom may form first as primary reaction products. Consequently, $CH_3 + OH$, $CH_3 + O$, $CH_2 + OH$, $CH_2 + O$ reactions may occur first leading to the formation of radical and stable species. In such a situation oxygen bearing species such as alcohols and aldehydes can be formed through processes involving fragments from methane and water.

We notice from Fig. 3 that counter to the IR signals of alka[e]nes whose spectral shapes and intensities are water independent, those corresponding to oxygen bearing spe-

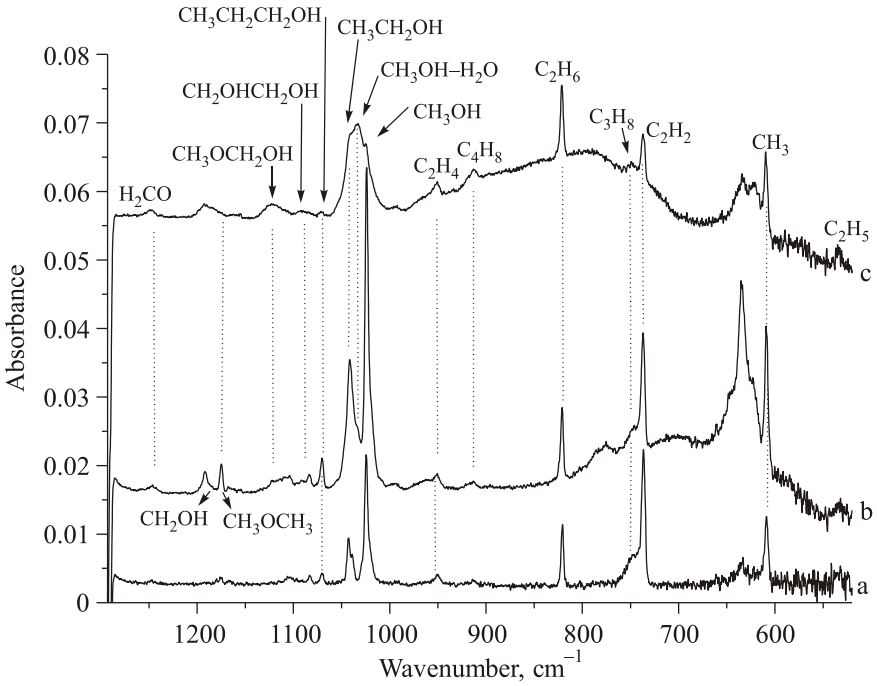

Fig. 3. Zoom in 1300–500 cm^{-1} spectral region of the difference spectra before and after UV photolysis of CH_4-rich ices containing H_2O formed at 3 K, with CH_4:H_2O concentration equal to 200:1 (a), 6:1 (b), 3:1 (c).

cies depend strongly in the amount of H_2O trapped in CH_4 matrix. In relatively diluted samples (Figs. 3(a) and 3(b)) the IR signals of the oxygenated photoproducts are clearly visible and well resolved. They become wider by increasing the water concentration in the sample (Fig. 3(c)). Accordingly, Figs. 3(a) and 3(b) allow the identification of oxygen bearing reaction products through their absorption bands which are clearly well defined and located at 1024.4, 1041.6, 1070.3, 1084.1, 1124.1, 1174.9, 1191.8, 1246.7 cm^{-1}.

The C–O stretching absorption peaks of alcohols are intense and normally fall between 1200 and 1000 cm^{-1}. Consequently, the peaks at 1024.4, 1041.6, 1070.3 cm^{-1} can be assigned to the C–O stretching mode of CH_3OH, CH_3CH_2OH, $CH_3CH_2CH_2OH$, respectively. The IR characterizations of solid CH_3OH, CH_3CH_2OH in different environments, have been investigated by many groups. Moore and Hudson [11] for example measured the characteristic IR signal of CH_3OH and CH_3CH_2OH trapped in CH_4–H_2O ice at 1020 and 1047 cm^{-1}, respectively, which is in good agreement with our assignments, concerning methanol and ethanol.

It is important to notice that among those absorption peak which may correspond to photoproducts trapped in CH_4–H_2O environments, some would be due to hydrated complexes where a photoproduct is complexed to water such as CH_3OH–H_2O wish are formed in samples with relative high amounts of water. This point will be discussed below concerning the H_2CO and H_2CO–H_2O detection. However, the matrix isolation study carried out by Bakkas *et al.* [23] showed that the C–O stretching absorption peaks of CH_3OH is bleu shifted by 13 cm^{-1} in hydrated methanol. This suggests that under our experimental conditions CH_3OH–H_2O would absorb at 1033 cm^{-1}. Such a peak is not observed in Fig. 3(a) where the amount of water is not high enough to form hydrated complexes. In the difference spectra of Figs. 3(b) and 3(c) a new peak appears at 1033 cm^{-1}, confirming the fact that hydrated complexes may be present under our experimental conditions only in samples with high amount of water (Figs. 3(b), (c)). From these observations, we have checked systematically the absorption peaks related to the reaction products and those related to hydrated reaction products.

As mentioned earlier, the IR identification of CH_3OH and CH_3CH_2OH has been based on previous studies [11–23], however, propanol has been less studied and for this reason, we have investigated the behavior of the spectral position shifts of the C–O stretching vibration of CH_3OH, CH_3CH_2OH and $CH_3CH_2CH_2OH$ in solid phase. In fact, as it will be discussed below, we have measured the C–O stretching peaks positions of solid CH_3OH, CH_3CH_2OH, $CH_3CH_2CH_2OH$ at 1023.8, 1045.7, 1067.9 cm^{-1}, respectively. This allows us to attribute the absorption peak at 1070.3 cm^{-1} to propanol. The analysis to the IR intensities of these 3 peaks showed that these alcohols are formed with an IR intensity distribution CH_3OH: CH_3CH_2OH: $CH_3CH_2CH_2OH$ = 10:4:1. The heating of the sample or the increasing of water amount in methane ice, as shown in Fig. 3(c), lead to an overlapping of these three IR signals, resulting in a wide absorption band centered around 1035 cm^{-1} and expanded between 1077 and 988 cm^{-1}. As the photolysis of CH_4 leads to the formation of long carbon chain species such as C_2H_6 and C_3H_8, naturally the adding of small amounts of water leads to the formation of the three

alcohols we mentioned, probably through the subsequent mechanisms:

Formation of CH_3OH

$$CH_3 + OH \rightarrow CH_3OH,$$
$$CH_3O + H \rightarrow CH_3OH,$$
$$CH_2OH + H \rightarrow CH_3OH.$$

Formation of CH_3CH_2OH

$$C_2H_5 + OH \rightarrow CH_3CH_2OH,$$
$$CH_3CH_2O + H \rightarrow CH_3CH_2OH,$$
$$CH_3 + CH_2OH \rightarrow CH_3CH_2OH.$$

Formation of $CH_3CH_2CH_2OH$

$$C_3H_7 + OH \rightarrow CH_3CH_2CH_2OH,$$
$$CH_3CH_2CH_2O + H \rightarrow CH_3CH_2OH,$$
$$CH_3CH_2 + CH_2OH \rightarrow CH_3CH_2OH.$$

Among all these mechanisms, those involving CH_3, C_2H_5, CH_3O and CH_2OH radicals are very probable as the four radicals have been observed experimentally under our experimental conditions. We have measured the spectral positions of CH_3 and C_2H_5 at 609.2 and 532.6 cm^{-1}, respectively, which is in good accordance with previous studies [4,5,14] concerning the fragmentation of methane ice. Another band at 1385.3 cm^{-1} (Fig. 4) behaves similarly as the bands at 609.2 and could also be due to the radical species CH_3. We have assigned, based on water concentration effects and sample heating, the peak at 1191.8 cm^{-1} to CH_2OH radicals (Fig. 3). Previous experimental studies involving radiation induced processing of H_2CO and CH_3OH ices have shown the formation of CH_2OH through its most intense IR signal around 1190 cm^{-1} [24,25], while CH_3O, probably more reactive, has not been detected.

The experimental observation of radicals would suggest that complex organic molecules other than CH_3OH, CH_3CH_2OH and $CH_3CH_2CH_2OH$ may be formed trough radical-radical recombination such as $CH_3O + CH_3$ to form CH_3OCH_3, $CH_3O + CH_2OH$ to form CH_3OCH_2OH or $CH_3O + CH_3O$ to form CH_3OOCH_3. The most intense IR signals characterizing CH_3OCH_3, CH_3OCH_2OH and CH_3OOCH_3, have been reported by several groups to be located at 1173, 1125 and 1032 cm^{-1} [26,27]. We have observed under our experimental conditions tow IR signals located at 1174.9 and 1124.1 cm^{-1} which may be assigned to CH_3OCH_3 and CH_3OCH_2OH, respectively. We notice that the IR signals at 1174.9 cm^{-1} characterizing CH_3OCH_3 is much higher than that at 1124.1 cm^{-1}, assigned to CH_3OOCH_3, indicating that species with one oxygen atom are probably formed more efficiently than species involving tow oxygen atoms. CH_3OOCH_3 species cannot be experimentally characterized as its most intense IR signal at 1032 cm^{-1} falls in the same spectral region as methanol and ethanol.

Finally, the two peaks detected at 1246.7 and 1084.1 cm^{-1} from Fig. 3 have been assigned to H_2CO and CH_2OHCH_2OH. These two species have been identified in irradiated CH_3OH and CH_4–CO ices [28,29] at 1246 and 1088 cm^{-1}, respectively. In these previous studies H_2CO has been characterized by three characteristic absorption signals at 1726, 1499 and 1246 cm^{-1}. We also observe, under our experimental conditions these three signals at 1736.2, 1495.5 and 1246.7 cm^{-1}, as shown in Figs. 3, 4 and 5. These three peaks are assigned to H_2CO as they behave similarly when the sample is heated or when the CH_4 and H_2O concentrations change.

Figure 5 shows the spectral region for the C=O functional group in radical species such as HCO which absorbs

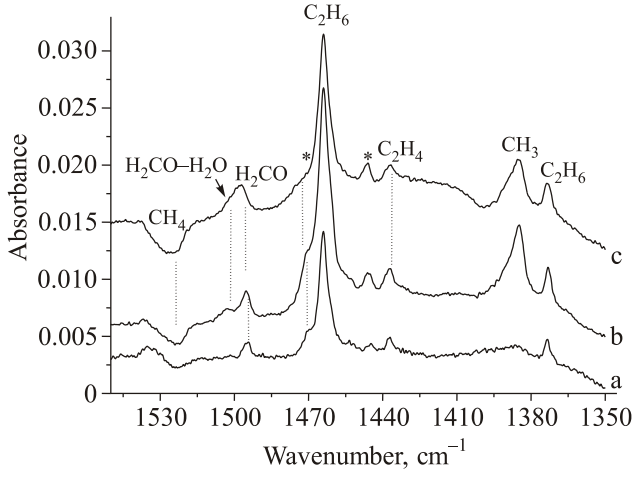

Fig. 4. Zoom in 1500–1300 cm^{-1} spectral region of the difference spectra before and after UV photolysis of CH_4-rich ices containing H_2O formed at 3 K, with CH_4:H_2O concentration equal to 200:1 (a), 6:1 (b), 3:1 (c); (*) not identified oxygenated species. The negative signal is due to CH_4 decrease during the ice photolysis.

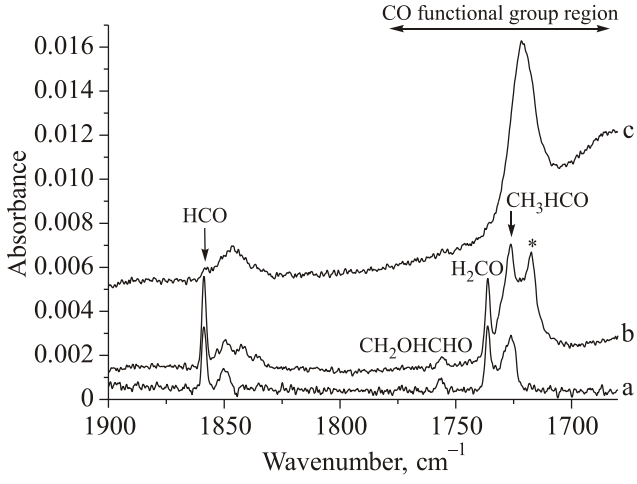

Fig. 5. Zoom in 1900–1650 cm^{-1} spectral region of the difference spectra before and after UV photolysis of CH_4-rich ices containing H_2O formed at 3 K, with CH_4:H_2O concentration equal to 200:1 (a), 6:1 (b), 3:1 (c); (*) band due to contributions from CH_3COCH_3, CH_3OCHO and hydrated aldehydes.

around 1860 cm^{-1} and stable molecules like the aldehydes H_2CO and CH_3CHO whose absorption bands are located round 1720 cm^{-1}. In this context Kaiser *et al.* [29] investigated the irradiation of CH_4–CO ice to monitor the formation of complex organics with C=O group through the analysis of a wide absorption band detected at 1727 cm^{-1}. They showed, using a deconvolution of the observed C=O functional group absorption band, that irradiation of CH_4–CO ice may lead to the formation of $HOCH_2CHO$, CH_3CH_2CHO, H_2CO, CH_3CHO, CH_3OCHO which would absorb at 1743, 1746, 1727, 1726, 1714 cm^{-1}, respectively.

Figure 5 shows that, under our experimental conditions, the band corresponding to the C=O functional group depends strongly on the amount of water in CH_4 ice. It becomes wide and unresolved for samples with CH_4:H_2O concentration equal to 3:1 (Fig. 5(c)).

In the infrared spectra corresponding to the lowest concentration of water (Fig. 5(a)), as there is no enough water to form hydrated species at 3 K, we distinguish three absorption peaks at 1756.4, 1736.2, 1726.4 cm^{-1}, which can be assigned to CH_2OHCHO, H_2CO, CH_3CHO, respectively. The identification of H_2CO and CH_3CHO is obvious as the peak at 1736.2 assigned to H_2CO correlates with other IR signals characteristic to H_2CO observed at 1495.5 and 1246.7 cm^{-1} shown in Figs. 3 and 4. On the other hand, Kaiser *et al.* showed that CH_3CHO trapped in methane ice [29] is characterized by its intense IR signal located at 1728 cm^{-1}. The peak detected at 1756.4 cm^{-1} shows a vibration frequency higher than 1740 cm^{-1} and it can be assigned to CH_2OHCHO.

Bennett *et al.* [30] reported the spectral position of CH_2OHCHO at 1757 cm^{-1} in irradiated methanol–carbon monoxide ice experiment. Previous studies [31] have reported the spectral positions of the C=O functional group in CH_2OHCHO ice at 1747 cm^{-1}.

The peak observed at 1756.4 cm^{-1}under our experimental conditions could also be due to aldehydes with alkyl groups ($C_nH_{2(n)+1}$ with $n > 1$). In fact Kaiser *et al.* [29] showed that to saturated aldehydes with alkylfunctional groups such as propanal (C_2H_5CHO) and butanal (C_3H_7CHO) trapped in CH_4 matrix show IR absorption signal with frequencies in the 1740–1750 cm^{-1} range, while ketones with alkyl groups such as acetone (CH_3COCH_3) absorb in lower frequency range around 1717 cm^{-1}.

We have recently reported [32] the CO group spectral positions in CH_3CH_2CHO and CH_3OCHO ices at 1729 and 1711 cm^{-1}, respectively. This suggests that the peak observed at 1717.4 cm^{-1} (Fig. 4(b)) would be due to either CH_3COCH_3 or CH_3OCHO. However we think that species with one oxygen are more probable under our experimental conditions. As shown in Figs. 5(b) and 5(c), the signal at 1717.3 cm^{-1} overlaps with the IR signal of the aldehydes trapped in samples with high amount of water and consequently part of this signal could be due to hydrated aldehydes. In Fig. 5(c) the wide absorption band due the aldehydes interacting with water is centered at 1721.5 cm^{-1} with a signal extended from 1800 to 1650 cm^{-1}. All these complex organic molecules formed under pour experimental conditions involve CHO fragment and might form through the following reactions:

$$H + HCO \rightarrow H_2CO,$$
$$CH_3 + HCO \rightarrow CH_3CHO,$$
$$CH_3O + HCO \rightarrow CH_3OHCO,$$
$$HOCH_2 + HCO \rightarrow HOCH_2CHO,$$
$$CH_3CH_2 + HCO \rightarrow CH_3CH_2CHO.$$

Species such as H_2CO and CH_3CHO may be formed trough processes such as H + HCO and H + CH_3CO which involve radical species with CO functional group. Many of these radical species absorb around 1860 cm^{-1}. The analysis of the IR signal in this spectral region shows that the absorption band is water concentration dependent. In Fig. 5(b) corresponding to a sample with relative high amount of water we distinguish 4 components located at 1858.8, 1849.4, 1842.4 and 1834.8 cm^{-1}. In samples with low concentration of water (Fig. 5(a)), we distinguish 2 absorption peaks at 1858.8 and 1849.4 cm^{-1} while in Fig. 5(c) corresponding to samples with huge amount of water the observed band is wide and centered at 1846.1 cm^{-1}.

All these IR signals located between 1860 and 1830 cm^{-1} may be due to radical species such as HCO, CH_3CO, HOCO or to hydrated HCO. HCO has been measured at 1842 and 1846 cm^{-1} in previous studies devoted to irradiation of H_2CO and CH_3OH ices [28,33], respectively. CH_3CO, HCO and HOCO trapped in argon matrix [24,34] have been observed at 1875, 1864 and 1843 cm^{-1}, respectively.

As mentioned earlier, the goal of the present work is to have an IR spectrum of heavy oxygenated species which would formed through the photo-induced solid state reaction involving H_2O and CH_4. Table 1 gathers a tentative assignment of species formed and trapped in methane ice at 3 K. The three spectral regions we have chosen to analyze are the only regions which are less perturbed by the IR signals of the reactants H_2O and CH_4 and the photoproducts proper to CH_4 fragmentation such as C_2H_6 which is formed efficiently under our experimental conditions. The 1500–1300 cm^{-1} and 3020–2500 cm^{-1} spectral regions, corresponding respectively to the CHC bending and CH stretching modes of many alcohols and alkanes, are dominated by the IR signal due to CH_4, C_2H_6 and C_2H_4 species which may hide the oxygen organics signals. In order to overcome such a problem we have heated the irradiated samples to be certain that all the alka[e]nes (C_xH_y) species are desorbed from our samples. It is important to notice that all alka[e]nes desorb at temperatures lower than 80 K while the alcohols and aldehydes desorb at temperatures higher than 100 K. We have then heated the irradiated CH_4–H_2O ices to 110 K for a new IR analysis of our irradiated heated samples.

Table 1. Tentative assignments of the IR signals detected during the VUV Photolysis of CH_4–H_2O mixture at 3 K

Reaction product	Spectral position, cm^{-1}		
	Present work	Literature	References
CH_3OH	1024.4	1020	[11]
CH_3OH–H_2O	1033.0	1033	[23]
CH_3CH_2OH,	1041.6	1047	[11]
$CH_3CH_2CH_2OH$	1070.3	1068	*
CH_2OHCH_2OH	1084.1	1088	[28,29]
CH_3OCH_2OH	1124.1	1125	[26,27]
CH_3OCH_3	1174.9	1173	[26,27]
CH_2OH	1191.8	1190	[24,25]
H_2CO	1246.7	1246	[28,29]
H_2CO	1495.5	1499	[28,29]
CH_3COCH_3	1717.4	1717	[29]
CH_3CHO	1726.4	1728	[29]
H_2CO	1736.3	1726	[28,29]
HCO	1846.1	1846	[28,33]
CH_2OHCHO	1756.4	1757	[30]

Notes: * The C–O stretching peak IR position of solid $CH_3CH_2CH_2OH$ has been measured in our lab.

Figure 6 shows the results of the heating to 110 K of the irradiated methane rich ices containing different amount of water. As mentioned in the introduction part, all the laboratory simulations of energetic processing of CH_4–H_2O mixed ices, have been carried out in water-rich environments in order to provide significant data correlating to observations. However such simulations cannot reveal the nature of all chemical species formed during the photo-induced irradiation of CH_4–H_2O mixed ices. This is only because of the huge wide absorption bands of water ice which hide many reaction products. In order to avoid such a problem, we have to reduce the absorption signal due to water ice. The analysis of the IR spectra from Fig. 6 shows that even under our experimental conditions which use CH_4-rich ices with relative low concentration of water trapped in solid methane (Fig. 6(a): 33% of H_2O in CH_4, Fig. 6(b): 17% of H_2O in CH_4) the heating of the irradiated sample to 110 K to remove all alka[e]nes leads to wide absorption bands due to water ice where CH_4 and reaction products remain trapped in water ice (Figs. 6(a) and 6(b)). From these two figures, we can distinguish signals due to, C–O vibration of alcohols around 1000 cm^{-1}, to C=O functional group around 1700 cm^{-1}, and to HCH bending and C–H stretching modes of alcohols and alkanes around 1300 and 3000 cm^{-1}, respectively. Such conditions cannot help with indentifying the oxygen bearing species formed through CH_4+H_2O solid state photo-induced reaction. The situation is completely different when the very diluted samples (Figs. 6(c) and 7(a): 0.5% of H_2O in CH_4) are heated to 110 K. The heating of such irradiated CH_4–H_2O ices allows to remove all alka[e]nes, including CH_4 and the IR signal due to H_2O ice is low enough to allow a better identification of the complex organic molecules formed through VUV photolysis of

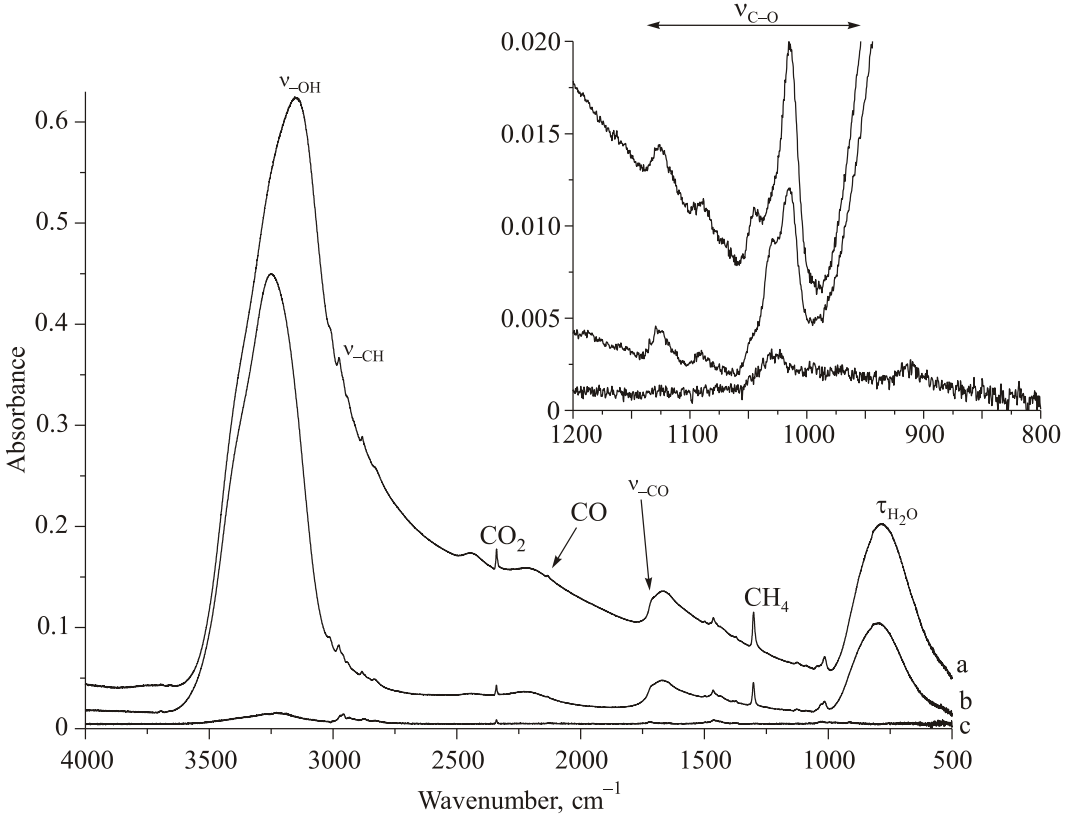

Fig. 6. (a) CH_4 + H_2O (3:1) ice after UV photolysis heated to 110 K; (b) CH_4 + H_2O (6:1) ice after UV photolysis heated to 110 K; (c) CH_4 + H_2O (200:1) ice after UV photolysis heated to 110 K. Top right: zoom of the figure in the 1200–800 cm^{-1} spectral region.

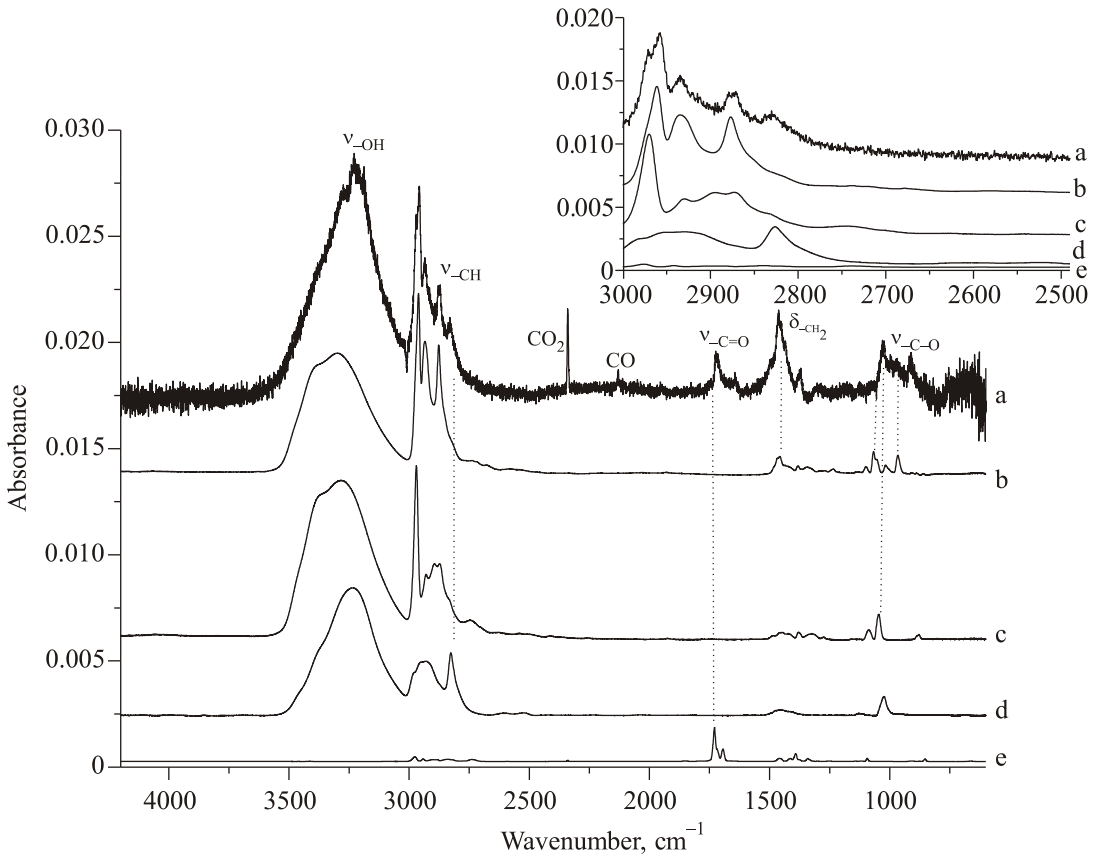

Fig. 7. CH_4 + H_2O (200:1) ice after UV photolysis heated to 110 K (a). Reference spectrum of solid $CH_3CH_2CH_2OH$ (b) CH_3OH (c), CH_3CH_2OH (d), solid CH_3CH_2CHO (e). Top right: zoom of the figure in the 3000–2600 cm^{-1} spectral region.

CH_4–H_2O. Figure 7 shows the IR spectra of the UV irradiated ice CH_4:H_2O (200:1) heated to 110 K, compared to the reference spectra of some organic molecules.

The IR spectrum of the heated irradiated methane-rich ice containing 0.5% of water contains IR signatures characteristic of organic molecules having OH, CH, C=O and C–O functional groups. All the species we have proposed to form under our experimental conditions at 3 K may fit the IR signatures of the resulting spectrum shown in Fig. 7(a). The IR signal due to the C=O functional group is wide and it is located in 1790–1600 cm^{-1} range. It shows a maximum at 1725 cm^{-1} with two components at 1750 and 1660 cm^{-1}. Due to the C=O functional group, many large aldehydes and even acids have intense IR signals in this spectral region. Similarly, the IR signal in the C–O stretching spectral region to characterize alcohols, is located in 1140–780 cm^{-1} spectral range, showing a first maximum at 1027 cm^{-1}, and another one at 911 cm^{-1}. In the CH spectral region, we notice from Fig. 7(a) a structure of 6 peaks at 2971, 2963, 2958, 2934, 2874 and 2831 cm^{-1}. Such a structure is indicative to the presence in the sample of alcohols larger than methanol and ethanol such as propanol.

We have limited the comparison of the IR spectrum of the heated irradiated methane-rich ice to a few IR reference spectra of long chain carbon species containing one oxygen atom: CH_3OH, CH_3CH_2OH, $CH_3CH_3CH_2OH$, and CH_3CH_2CHO. The comparison of all these reference spectra to our experimental spectrum shows that in addition to small organics such as H_2CO, CH_3CHO, CH_3OH and CH_3CH_2OH already identified in previous CH_4–H_2O irradiation experiments, at least two large complex organic molecules such as propanal and propanol may be formed in ice mixtures containing water and methane and exposed to energetic sources. In previous experiments related to the irradiation of H_2O–CH_4 mixed ices in water-rich environments only CH_3OH, C_2H_5OH, H_2CO, CH_3CHO in addition to CO and CO_2 have been experimentally observed as oxygenated reaction products.

The formation of alcohols such as CH_3OH, CH_3CH_2OH, $CH_3CH_3CH_2OH$ derived from the corresponding alkanes CH_4, C_2H_6 and C_3H_8 may take place through two different mechanisms involving either O or OH fragments. Consequently, the role of water into the chemical evolution of H_2O + CH_4 UV-induced reaction depends on the water fragment involved in the processing. Dissociated into H and OH, H_2O may play a catalytic role as for each water fragmentation, a regenerated H_2O may form through H abstraction reaction from methane as follows:

$$H_2O + h\nu \rightarrow OH + H,$$
$$CH_4 + OH \rightarrow CH_3 + H_2O.$$

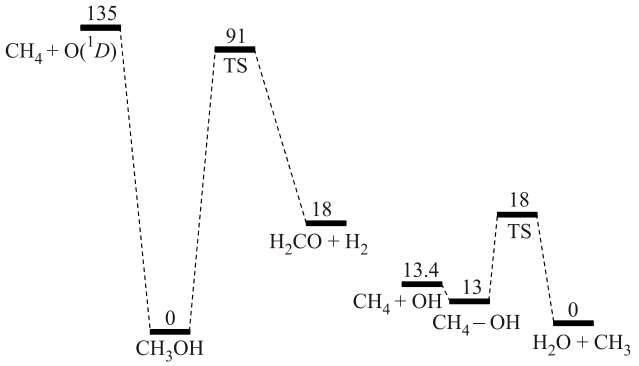

Fig. 8. Energy diagrams (kcal/mol) involving $O(^1D)$ + CH_4 and OH + CH_4 reactions, based on theoretical investigations carried out by Tsiouris *et al.* [35] and Chang *et al.* [36]. TS: transition states.

The CH_4 + OH reaction is exothermic with a very low activation energy [35]. This shows that water present even as traces in methane ice may contribute indefinitely, through successive H_2O regeneration (CH_4 + OH → CH_3 + H_2O), into the chemical transformation of methane during and even after ice irradiation.

Water may also dissociate into H_2 + O and in such a situation atomic oxygen in its excited state $O(^1D)$ would react with methane to form either CH_3OH and H_2CO through oxygen insertion reaction into C–H bond. The reaction is barrierless and highly exothermic [36] which allows the formation of both methanol and fragments from methanol such as H_2CO:

$$H_2O + h\nu \rightarrow O^* + H_2,$$
$$CH_4 + O^* \rightarrow CH_3OH \text{ or } CH_3OH^*,$$
$$CH_3OH^* \rightarrow H_2CO + H_2.$$

Figure 8 shows two-energy diagrams involving OH + CH_4 and $O(^1D)$ + CH_4 reactions, based on theoretical investigations carried out by Tsiouris *et al.* [35] and Chang *et al.* [36], respectively. Such processing involving either O and OH fragments from water and one methane molecule may be extended to all the hydrocarbons formed during the photolysis of CH_4 such as C_2H_6, C_2H_8 which react efficiently with OH through hydrogen abstraction reactions. Overend *et al.* [37] measured in gas phase the rate constants of hydrogen abstraction from CH_4, C_2H_6 and C_3H_8 at $3.9\cdot10^9$, $1.6\cdot10^{11}$ and $1.2\cdot10^{12}$ $cm^3\cdot mol^{-1}\cdot s^{-1}$. Accordingly large linear alcohols involving radical alkyl, R:CH_3, C_2H_5, C_3H_8 may form through the following two steps reactions:

$$RH + OH \rightarrow R^\circ + H_2O,$$
$$R^\circ + OH \rightarrow ROH.$$

Conclusion

In the interstellar medium as well as in our solar system, the UV-induced solid state chemistry of methane may be the source of many carbon chain complex organic molecules. As the chemical composition of many solar system and interstellar icy bodies are found to be dominated by H_2O, the photochemistry of methane has been investigated by several groups in water-rich ices in order to investigate, using IR spectroscopy, the oxygen bearing organics synthesis. Although these investigations are carried out to provide significant data correlating to the astronomical observations, they cannot reveal the nature of all the chemical species formed during the photo-processing of CH_4–H_2O mixed ices. The huge wide absorption bands of water ice hiding many reaction products might be an hindrance to really characterize the CH_4 + H_2O photo-induced solid state reaction. We have shown in the present work the role played by water molecules in the photo-decomposition of solid methane and revealed that photoproducts formed in solid phase upon VUV irradiation of CH_4–H_2O mixture may be the source of very large complex molecules. The analysis of our IR spectra shows that the presence of water molecules even as traces in solid methane influences considerably its photochemistry at cryogenic temperatures. We show that in CH_4-rich environments both alka[e]nes such as C_2H_6, C_2H_4, C_2H_2, C_3H_8, CH_3 and C_2H_5 and large oxygen bearing organics such as H_2CO, CH_3CHO, CH_3CH_2CHO, CH_2OHCHO, CH_3OH, CH_3CH_2OH, CH_3OCH_3, CH_2OHCH_2OH are efficiently formed at temperatures as low as 3 K. However while the IR signatures of the alka[e]nes species C_xH_y dominate the IR spectra of the irradiated CH_4–H_2O ices at temperatures lower than 50 K, the heating of the samples to 110 K reveals the formation of large carbon chain complex organic molecules having OH, CH, C=O and C–O functional groups and whose IR absorption signals are not perturbed nor shaded by the IR signals of water ice.

Acknowledgment

This work was supported in part by the LabEx MiChem "French state funds managed by the ANR within the Investissements d'Avenir programme under reference ANR-11-IDEX-0004–02." We thank also the Program PCMI (INSU–CNRS) for funding support.

1. E.J.R. Parteli, J. Radebaugh, R.A. Beyer, T. Bertrand, F. Forget, F. Nimmo, W.M. Grundy, J.M. Moore, S.A. Stern, J. Spencer, T.R. Lauer, A.M. Earle, R.P. Binzel, H.A. Weaver, C.B. Olkin, L.A. Young, K. Ennico, and K. Runyon, *Science* **360**, 992 (2018).
2. E.L. Barth Owen, and B. Toon, *Icarus* **182**, 230 (2006).

3. Y.J. Wu, H.F. Chen, C. Camacho, H.A. Witek, S.C. Hsu, M.Y. Lin, S.L. Chou, J.F. Ogilvie, and B.M. Cheng, *Astrophys. J.* **701**, 8 (2009).
4. M.Y. Lin, J.I. Lo, H.C. Lu, S.L. Chou, Y.C. Peng, B.M. Cheng, and J.F. Ogilvie, *J. Phys. Chem. A* **118**, 3438 (2014).
5. C.J. Bennett, C.S. Jamieson, Y. Osamura, and R.I. Kaiser, *Astrophys. J.* **653**, 792 (2006).
6. K. Kobayashi, W.D. Geppert, N. Carrasco, N.G. Holm, O. Mousis, M.E. Palumbo, J.H. Waite, N. Watanab, and L.M. Ziurys, *Astrobiology* **17**, 8 (2017).
7. A. Bergantini, P. Maksyutenko, and R.I. Kaiser, *Astrophys. J.* **841**, 96 (2017).
8. B. Tercero, I. Kleiner, J. Cernicharo, H.V.L. Nguyen, A. López, and G.M. Muñoz Caro, *Astrophys. J. Lett.* **770**, 13 (2013).
9. N. Brouillet, D. Despois, A. Baudry T.-C. Peng, C. Favre, A. Wootten, A.J. Remijan, T.L. Wilson, F. Combes, and G. Wlodarczak, *Astronomy & Astrophysics A* **46**, 550 (2013).
10. M.H. Moore and R.L. Hudson, *IAU Colloquium.* **231**, 119 (2005).
11. M.H. Moore and R.L. Hudson, *Icarus* **135**, 518 (1998).
12. D. Bockelée-Morvan, J. Crovisier, S. Erard, F. Capaccioni, C. Leyrat, G. Filacchione, P. Drossart, T. Encrenaz, N. Biver, M.-C. de Sanctis, B. Schmitt, E. Kuhrt, M.-T. Capria, M. Combes, M. Combi, N. Fougere, G. Arnold, U. Fink, W. Ip, A. Migliorini, G. Piccioni, and G. Tozzi, *MNRAS* **462**, S183 (2016).
13. M. Jonusas, and L. Krim, *MNRAS* **470**, 4564 (2017)
14. F.A. Vasconcelos, S. Pilling, W.R.M. Rocha, H. Rothard, P. Boduch, and J.J. Ding, *Phys. Chem. Chem. Phys.* **19**, 12845 (2017).
15. O.N. Ulenikov, E.S. Bekhtereva, S. Albert, S. Bauerecker, H.M. Niederer, and M. Quack, *J. Chem. Phys.* **141**, 234302 (2014).
16. A. Mencos, S. Nourry, and L. Krim, *MNRAS* **467**, 2150 (2017).
17. P.A. Gerakines, W.A. Schutte, J.M. Greenberg, and E.F. van Dishoeck, *Astronomy & Astrophysics* **296**, 810 (1995).
18. J. Ceponkus, P. Uvdal, and B. Nelande, *J. Phys. Chem. A* **112**, 3921 (2008).
19. P.A. Gerakines, J.J. Bray, A. Davis, and C.R Richey, *Astrophys. J.* **620**, 1140 (2005).
20. R. Luna, M.A. Satorre, M. Domingo, C. Millán, and C. Santonja, *Icarus* **221**, 186 (2012).
21. K. Yamakawa, N. Ehara, N. Ozawa, and I. Arakawa, *AIP Adv.* **6**, 75302 (2016).
22. R.E. Johnson, and T.I. Quickenden, *J. Geophys. Res.* **102**, 10985 (1997).
23. N. Bakkas, Y. Bouteiller, A. Loutellier, J.P. Perchard, and S. Racine, *J. Chem. Phys.* **99**, 3335 (1993).
24. T. Butscher, F. Duvernay, P. Theule, G. Danger, Y. Carissan, D. Hagebaum-Reignier, and T. Chiavassa, *MNRAS* **453**, 1587 (2015).
25. E.V. Saenko, and V.I. Feldman, *Phys. Chem. Chem. Phys.* **18**, 32503 (2016).
26. K.O. Christe, *Spectrochim. Acta*, *Part A* **27**, 463 (1971).
27. R. Wrobel, W. Sander, E. Kraka, and D. Cremer, *J. Phys. Chem. A* **103**, 3693 (1999).
28. S. Maity, R.I. Kaiser, and B.M. Jones, *Phys. Chem. Chem. Phys.* **17**, 3081 (2015).
29. R.I. Kaiser, S. Maity, and B.M. Jones, *Phys. Chem. Chem. Phys.* **16**, 3399 (2014).
30. C.J. Bennett, and R.I. Kaiser, *Astrophys. J.* **661**, 899 (2007).
31. R.L. Hudson, M.H. Moore, and A.M. Cook, *ASR* **36**, 184 (2005).
32. L. Krim, M. Jonusas, J.-C. Guillemin, M. Ya, and A. Lamsabhi, *Phys. Chem. Chem. Phys.* **20**, 19971 (2018).
33. T. Butscher, F. Duvernay, G. Danger, and T. Chiavassa, *Astronomy & Astrophysics* **593**, A60 (2016).
34. P. Das, and Y.-P. Lee, *Chem. Phys*. **140**, 244303 (2014).
35. M. Tsiouris, M.D. Wheeler, and M.I. Lester, *Chem. Phys. Lett.* 302, 192 (1999).
36. A.H.H. Chang, and S.H. Lin, *Chem. Phys. Lett.* **384**, 229 (2004).
37. R.P. Overend, G. Paraskevopoulos, and R.J. Cvetanovic, *Can. J. Chem.* **53**, 3374 (1975).

ВУФ фотоліз суміші CH_4–H_2O в метанвмісних льодах: утворення великих складних органічних молекул в астрономічних середовищах

Lahouari Krim and Mindaugas Jonusas

Вивчено вплив молекул води на фотодеструкцію метанового льоду та утворення фотопродуктів в твердій фазі при ВУФ опроміненні суміші CH_4–H_2O в метанвмісних льодах. Аналіз ІЧ спектрів показує, що навіть при дуже низьких концентраціях води в метанових льодах утворюється ряд кисневмісних вуглеводнів, отриманих в результаті фоторозкладу води та метану при кріогенних температурах. Показано, що як алка[е]ни, так і кисневмісні органічні речовини ефективно утворюються при температурах до 3 К. Однак в той час як ІЧ характерні смуги алка[е]нів, таких як C_2H_6, C_2H_4 і C_2H_2, домінують в ІЧ спектрах опромінених льодів CH_4–H_2O при температурах нижче 50 К, нагрівання зразка до 110 К виявляє утворення органічних молекул з великими вуглецевими ланцюгами, таких як етанол, пропанол, пропанал та гліколевий альдегід.

Ключові слова: астрохімія, лабораторне моделювання, ІЧ спектроскопія, складні органічні молекули.

ВУФ фотолиз смеси CH_4–H_2O в метансодержащих льдах: образование крупных сложных органических молекул в астрономических средах

Lahouari Krim and Mindaugas Jonusas

Изучено влияние молекул воды на фотодеструкцию метанового льда и образование фотопродуктов в твердой фазе при ВУФ облучении смеси CH_4–H_2O в метансодержащих льдах. Анализ ИК спектров показывает, что даже при очень

низких концентрациях воды в метановых льдах образуется ряд кислородсодержащих углеводородов, полученных в результате фоторазложения воды и метана при криогенных температурах. Показано, что как алка[e]ны, так и кислородсодержащие органические вещества эффективно образуются при температурах до 3 К. Однако в то время как ИК характерные полосы алка[e]нов, таких как C_2H_6, C_2H_4 и C_2H_2, доминируют в ИК спектрах облученных льдов CH_4–H_2O при температурах ниже 50 К, нагрев образца до 110 К выявляет образование органических молекул с крупными углеродными цепями, таких как этанол, пропанол, пропанал и гликолевый альдегид.

Ключевые слова: астрохимия, лабораторное моделирование, ИК спектроскопия, сложные органические молекулы.